The RhoGEF protein Plekhg5 regulates medioapical and junctional actomyosin dynamics of apical constriction during *Xenopus* gastrulation

Austin Baldwin[a,†,*], Ivan K. Popov[b], Ray Keller[c], John Wallingford[a], and Chenbei Chang[b,†,*]
[a]Department of Molecular Biosciences, University of Texas at Austin, Austin, TX 78712; [b]Department of Cell, Developmental and Integrative Biology, University of Alabama at Birmingham, Birmingham, AL 35294; [c]Biology Department, University of Virginia, Charlottesville, VA 22903

ABSTRACT **Apical constriction results in apical surface reduction in epithelial cells and is a widely used mechanism for epithelial morphogenesis. Both medioapical and junctional actomyosin remodeling are involved in apical constriction, but the deployment of medial versus junctional actomyosin and their genetic regulation in vertebrate embryonic development have not been fully described. In this study, we investigate actomyosin dynamics and their regulation by the RhoGEF protein Plekhg5 in *Xenopus* bottle cells. Using live imaging and quantitative image analysis, we show that bottle cells assume different shapes, with rounding bottle cells constricting earlier in small clusters followed by fusiform bottle cells forming between the clusters. Both medioapical and junctional actomyosin signals increase as surface area decreases, though correlation of apical constriction with medioapical actomyosin localization appears to be stronger. F-actin bundles perpendicular to the apical surface form in constricted cells, which may correspond to microvilli previously observed in the apical membrane. Knockdown of *plekhg5* disrupts medioapical and junctional actomyosin activity and apical constriction but does not affect initial F-actin dynamics. Taking the results together, our study reveals distinct cell morphologies, uncovers actomyosin behaviors, and demonstrates the crucial role of a RhoGEF protein in controlling actomyosin dynamics during apical constriction of bottle cells in *Xenopus* gastrulation.**

Monitoring Editor
Rachel Brewster
University of Maryland, Baltimore County

Received: Sep 12, 2022
Revised: Mar 23, 2023
Accepted: Apr 6, 2023

INTRODUCTION

Apical constriction, an active process via which cells contract their apical surface, is one of the driving forces of epithelial morphogenesis (Sawyer *et al.*, 2010; Martin and Goldstein, 2014). Cells undergoing apical constriction often elongate their basolateral compartments and exert pulling forces on their neighbors. Apical constriction is used reiteratively during embryonic development to bend and fold epithelial sheets, such as during gastrulation movements in various animal species, folding of the neural ectoderm into a closed neural tube, lumen and tube formation during organogenesis, and sensory placode morphogenesis. Increasing our depth of understanding of the molecular machinery controlling apical constriction can therefore provide broad insight into epithelial remodeling crucial for embryogenesis.

Apical constriction is regulated by dynamic and spatially restricted reorganization of cytoskeleton networks (Martin and Goldstein, 2014). Both actomyosin and microtubules have been implicated in this process (Rogers *et al.*, 2004; Lee *et al.*, 2007; Lee and Harland, 2007; Booth *et al.*, 2014; Ko *et al.*, 2019; Le and Chung, 2021), though the roles of actomyosin have been investigated in more depth. Recruited to apical cell–cell junctions by adhesion

This article was published online ahead of print in MBoC in Press (http://www.molbiolcell.org/cgi/doi/10.1091/mbc.E22-09-0411) on April 12, 2023.

†These authors contributed equally.

*Address correspondence to: Austin Baldwin (atbaldwin@utexas.edu); Chenbei Chang (cchang@uab.edu).

Abbreviations used: Dia, diaphanous; F-actin, filamentous actin; GFP, green fluorescent protein; mem-mCherry, membrane mCherry; MLC, myosin light chain; MO, morpholino oligo; myoIIB, non-muscle myosin heavy chain IIB; SEM, scanning electron microscopy.

complexes, filamentous actin (F-actin) and its associated motor protein non–muscle type II myosin form a circumferential junctional belt that facilitates the establishment and maintenance of cell adhesion. Contraction of junctional actomyosin can lead to reduction of apical membrane size by a purse-string mechanism. Enhanced junctional actomyosin activity consistent with purse-string constriction has been observed in ectopic apical constriction induced by specific regulators in epithelial cell cultures, in wound healing responses, and in dorsal closure during *Drosophila* development (Bement *et al.*, 1993; Nakajima and Tanoue, 2011, 2012; Kamran *et al.*, 2017; Kiehart *et al.*, 2017; Yano *et al.*, 2021).

Recently, studies in multiple systems have revealed that apical constriction can also be mediated by assembly of actomyosin in the medial region of the apical cell cortex. The medioapical actomyosin undergoes dynamic remodeling and engages cell junctions to actively shrink the apical cell surface. This mechanism is utilized during *Drosophila* and *Caenorhabditis elegans* gastrulation as well as in multiple processes in *Drosophila* after gastrulation, in lens placode invagination, and in the neural plate cells during neural tube closure (Martin *et al.*, 2009; Martin and Goldstein, 2014; Blanchard *et al.*, 2010; Plageman *et al.*, 2011; Roh-Johnson *et al.*, 2012; Booth *et al.*, 2014; Lang *et al.*, 2014; Simões *et al.*, 2014, 2017; Christodoulou and Skourides, 2015; Jodoin *et al.*, 2015; An *et al.*, 2017; Chanet *et al.*, 2017; Chung *et al.*, 2017; Goldstein and Nance, 2020). A hybrid strategy of employing both junctional and medioapical actomyosin has also been observed during neuroblast ingression in *Drosophila* and apical constriction of neural ectoderm cells in *Xenopus* during neurulation (Simões *et al.*, 2017; Baldwin *et al.*, 2022a). Thus, apical constriction mechanisms are both varied and complex, and understanding mechanisms employed in particular processes will involve observing both medial and junctional actomyosin simultaneously.

One of the prominent examples of apical constriction is the formation of bottle cells during *Xenopus* gastrulation (Keller, 1981; Hardin and Keller, 1988; Kurth and Hausen, 2000; Kurth, 2005; Lee and Harland, 2007, 2010). Bottle cells reduce their apices, elongate along the apicobasal axis, and expand their basal compartments during gastrulation. Pigment granules concentrate underneath the apical cell membrane as the apical surface is reduced, making the appearance of darkly colored cells the hallmark of apical constriction during *Xenopus* gastrulation. The bottle cells initially form on the dorsal side of the embryo and subsequently spread toward lateral and ventral quadrants to form the blastopore lip. The change in morphology of bottle cells leads to invagination of surface epithelium that coordinates with tissue involution in the underlying mesoderm. When bottle cells are removed surgically or prevented from forming by gene manipulations, *Xenopus* embryos can still complete gastrulation through tissue involution at ectopic sites that buckle due to other morphogenetic movements. However, imprecision of the tissue involution sites often leads to embryonic defects, such as shortening of anterior archenteron and malformation of head structure (Keller, 1981; Hardin and Keller, 1988; Popov *et al.*, 2018). This highlights the importance of bottle cells in conferring precision and robustness of gastrulation movements.

Apical constriction of bottle cells is regulated by signals controlling mesendoderm cell fate and polarity, such as those of nodal and planar cell polarity (Kurth and Hausen, 2000; Choi and Sokol, 2009; Ossipova *et al.*, 2015). Our recent studies reveal that a RhoGEF gene, *plekhg5*, is transcriptionally activated by nodal signaling and is required for apical constriction induced by ectopic nodal expression in the animal region or in endogenous bottle cells (Popov *et al.*, 2018). Plekhg5 stimulates Rho activation and likely regulates actomyosin dynamics via Rho effectors, such as Diaphanous (Dia), which facilitates assembly of F-actin bundles, and ROCK, which activates myosin II through phosphorylation of regulatory myosin light chain (MLC [Mulinari *et al.*, 2008; Massarwa *et al.*, 2009; Mason *et al.*, 2013; Rousso *et al.*, 2013]). Analysis of F-actin and pMLC indeed shows that knockdown of *plekhg5* reduces their apical accumulation in presumptive bottle cells and prevents cell shape changes of bottle cells (Popov *et al.*, 2018). However, the behaviors of actomyosin in normal bottle cells and how they are altered in *plekhg5* knockdown embryos are not known.

In this study, we tackle the following questions. How is apical actomyosin remodeled during apical constriction of bottle cells? Do junctional, medioapical, or combined actomyosin activities drive apical surface reduction? What are the kinetics of actomyosin accumulation and apical surface reduction? And how does *plekhg5* regulate actomyosin dynamics in bottle cells? Using live cell imaging and quantitative image analysis approaches, we show that both medioapical and junctional actomyosin play roles in apical constriction of bottle cells and *plekhg5* regulates accumulation of F-actin and myosin without affecting initial F-actin dynamics. Our data address an important knowledge gap about cytoskeleton regulation by a RhoGEF protein during apical cell constriction of bottle cells in *Xenopus* gastrulation, an important developmental process in a vertebrate species.

RESULTS

Heterogeneous morphology of the bottle cells

Bottle cell morphology was first studied using scanning electron microscopy (SEM) in both en face and sagittal views, while molecular studies of bottle cell formation tend to rely on the appearance of surface pigmentation and side views of the bottle cell shape (Hardin and Keller, 1988; Kurth and Hausen, 2000; Lee and Harland, 2007, 2010; Choi and Sokol, 2009; Ossipova *et al.*, 2015). To examine apical cell morphology during bottle cell formation, we labeled the bottle cells by expressing an mRNA encoding membrane-mCherry (mem-mCherry) in the dorsal marginal zone cells. The surface of the labeled epithelial cells was examined at early gastrula stages by confocal microscopy. We observed that bottle cells displayed distinct morphologies. Clusters of small round cells (Figure 1A, yellow arrow) were often flanked by fusiform cells that displayed circumferential elongation with reduced animal–vegetal cell length (Figure 1A, blue arrow). The distinct cell shapes implied that bottle cells may undergo different constrictive behaviors that can result in the adoption of different cellular morphologies.

F-actin distribution across subcellular domains in the bottle cells

To investigate whether both junctional F-actin belts and medioapical F-actin networks supply the constrictive forces in the bottle cells, we coinjected mem-mCherry RNA with that of utrophin-GFP, which encodes the F-actin–binding protein utrophin conjugated with green fluorescent protein (GFP). The utrophin-GFP signal was seen primarily at the cell–cell junctions in nonconstricting (or not yet constricting) cells but enriched at the apical cell compartment in constricting bottle cells (Figure 1B). Side views of utrophin-GFP distribution revealed that the signal was not simply accumulated under the apical cell membrane but seemed to form discrete bundles perpendicular to the plasma membrane (Figure 1B, right panels). This "bundled" pattern appeared to be similar to the microvilli previously observed on the apical surface of the bottle cells by scanning and transmission electron microscopy studies (Keller, 1981; Hardin and Keller, 1988; Kurth and Hausen, 2000; Lee and Harland, 2010).

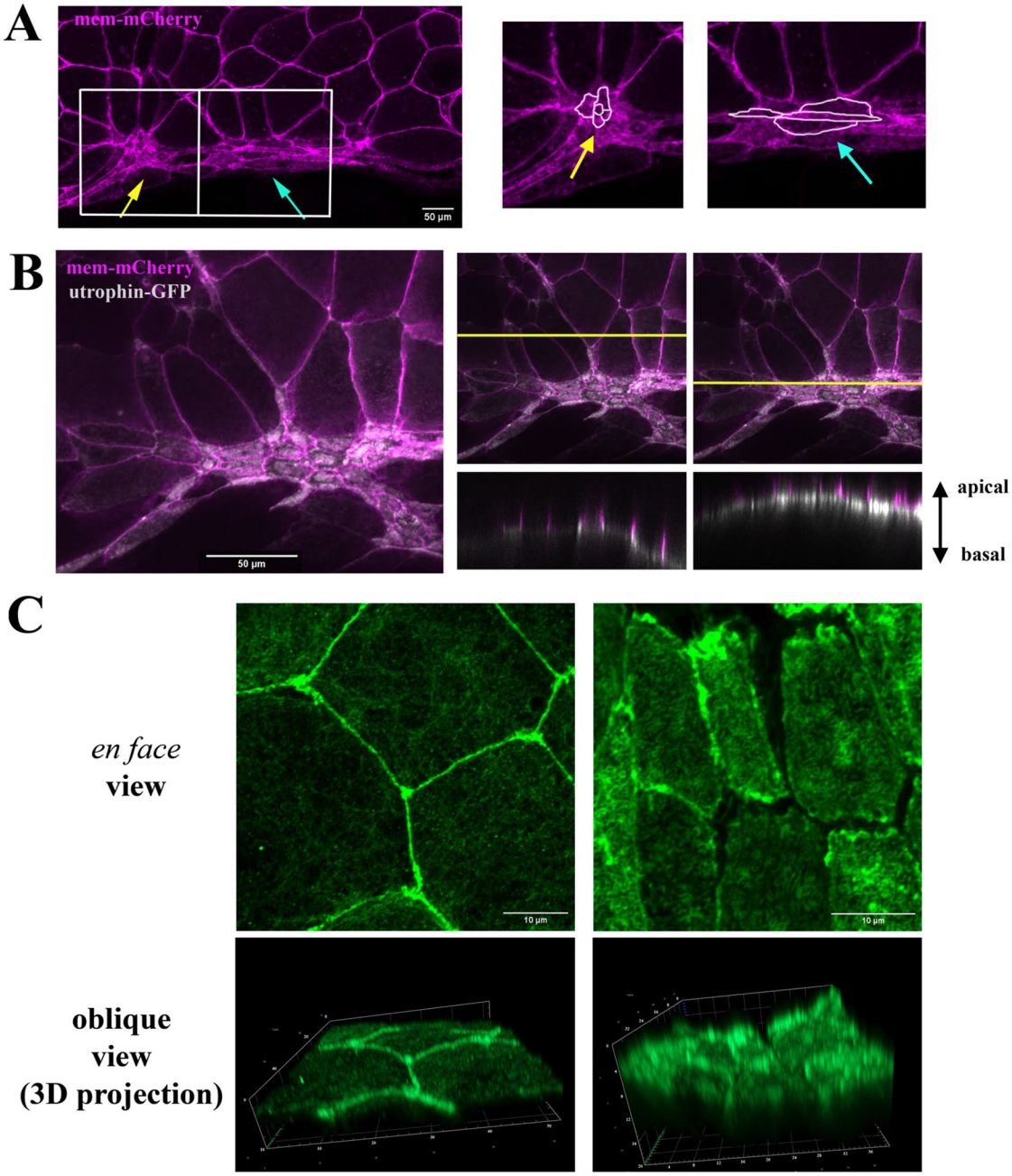

FIGURE 1: Distinct cell shapes, apical actin accumulation, and F-actin bundles in bottle cells. (A) Membrane mCherry–labeled bottle cells show two distinct morphologies, with round cells (yellow arrow) interspersed with fusiform cells (blue arrow). The panels on the right are the enlarged images of the boxed areas. (B) Coexpression of membrane mCherry with utrophin-GFP reveals accumulation of F-actin predominantly in the medial regions of apical cell cortex. The right two panels show the z-view of F-actin and mem-mCherry signals in regions without or with apical constriction. (C) En face images of phalloidin-stained fixed gastrula embryos show predominant cell junction localization of F-actin in not-yet-constricting cells (left top panel), whereas F-actin intensity is enhanced in the apical compartment of constricting cells (right top panel). Oblique views of 3D projections of the images reveal formation of dense F-actin bundles perpendicular to the apical surface in the constricting bottle cells (right bottom panel).

To further confirm the presence of F-actin bundles orthogonal to the cell surface, we examined F-actin patterns in fixed gastrula embryos stained with fluorescent dye–conjugated phalloidin. Oblique views of three-dimensional (3D)-projected Airyscan microscopy images revealed densely packed perpendicular F-actin bundles in the apical cortex of bottle cells. These F-actin bundles were longer in bottle cells that were more apically constricted (Figure 1C; Supplemental Figure 1). These results are consistent with the formation of previously-described actin-rich microvilli during bottle cell formation (Keller, 1981; Hardin and Keller, 1988; Kurth and Hausen, 2000; Lee and Harland, 2010) and imply that this may be a critical step in the reduction of the apical area.

Dynamic F-actin remodeling during bottle cell formation

To gain insight into F-actin dynamics during apical constriction of bottle cells, we performed live imaging of embryos coinjected with

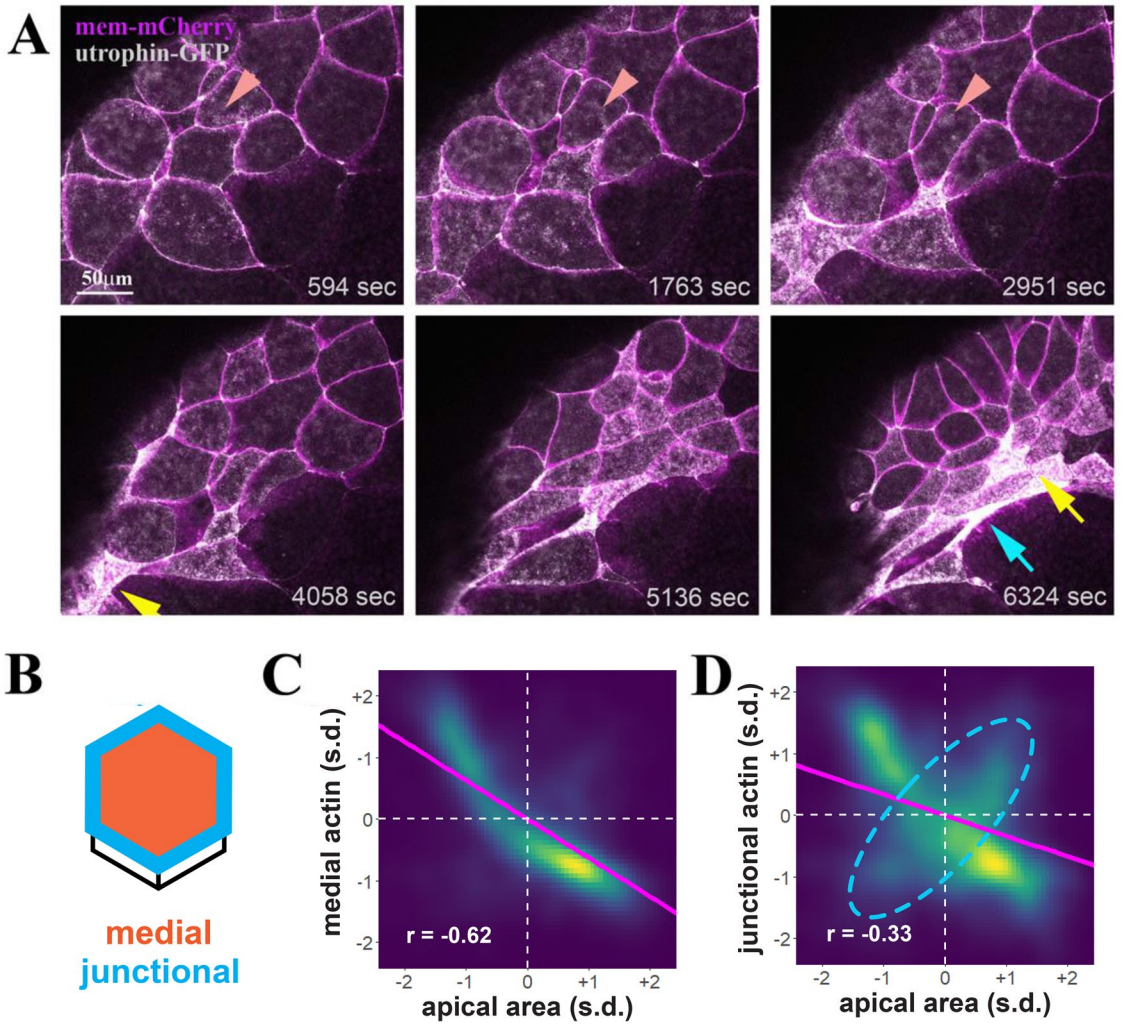

FIGURE 2: Dynamic F-actin remodeling accompanies apical surface reduction during bottle cell formation. (A) Selected frames from a time-lapse movie demonstrate dynamic F-actin organization before an overt decrease in apical cell area (top panels). The dynamic F-actin signal in a single cell is marked by the arrowheads. As apical constriction commences, groups of cells constrict first and take round shape (yellow arrow), with neighboring, later-constricting cells assuming fusiform (blue arrow). The clusters of round cells can appear as one large cell as cell constriction and F-actin signal increase often obscure cell boundaries (e.g., the cluster indicated by the yellow arrow at the 6324 s frame consists of five constricted cells seen in the time-lapse movie). (B) Schematics of quantification of medial (orange) and junctional (blue) F-actin intensity within single cells. (C, D) Density plots of apical cell area vs. medial (C) and junctional (D) F-actin. Magenta line indicates linear model. s.d. = standard deviations. *n* = 11,748 observations of 132 cells from four embryos. (C) A negative correlation of medial F-actin intensity and apical area is uncovered, with the correlation coefficient r value of –0.62. (D) Junctional F-actin intensity is also negatively correlated with the apical area, though less so with the r value of –0.33. This weaker correlation may be in part due to a subpopulation of cells with a positive correlation between junctional F-actin and the apical area (dashed cyan ellipsis).

mRNAs of mem-mCherry and utrophin-GFP (Supplemental Movies 1 and 2). Dynamic reorganization of F-actin puncta at the subapical cortex was visible before substantial reduction of the apical cell surface (Figure 2A, arrowheads, top panels). As the intensity of subapical F-actin was increased with time, the apical surface areas of cells were reduced. Given that we observed F-actin localization at both the apical junctions and medial apical surface, we examined whether F-actin localization at either subcellular domain correlated more strongly with apical constriction. We used Tissue Analyzer to segment the apical cell junctions of each cell in each frame and then delineate nonoverlapping medial and junctional apical domains for each cell (Figure 2B) (Aigouy *et al.*, 2010, 2016, 2020). This quantification revealed a strong negative correlation between mean medial F-actin localization and apical area (r = –0.62) (Figure 2C). A weaker negative correlation (r = –0.33) was observed between apical area and junctional F-actin localization (Figure 2D); this appears to be at least partly due to a population of cells where junctional actin and apical area are positively correlated (Figure 2D, dashed cyan ellipsis), indicating that the function of junctional F-actin in apical constriction may not be as consistent across the population of bottle cells as it is for medial F-actin. These results suggest that medial and junctional F-actin contractility may both play roles in apical constriction in the bottle cells, similar to that in the *Xenopus* neural ectoderm (Baldwin *et al.*, 2022a) but the role of junctional F-actin may be more variable across the population of bottle cells.

In generating movies of bottle cell apical constriction, we observed that apical constriction was initiated within clusters of cells

spaced some distance apart along the blastopore lip, with cells between the clusters constricting at later times (Supplemental Movies 1 and 2). The early constricting cells tended to have a round morphology, reflecting possible isotropic contraction forces (Figures 2A and 3A, yellow arrows). The cells between the clusters adopted a fusiform shape that appeared to be stretched by constricting neighboring cells in the clusters (Figures 2A and 3A, blue arrows; Supplemental Movies 1 and 2). Quantification of the changes in cell shape using the "stretch" parameter calculated by Tissue Analyzer (Aigouy *et al.*, 2010) (Figure 3B) showed that within a cluster of constricting cells, a small number of extremely constrictive cells became rounder (decreased stretch) while surrounding cells took on fusiform shapes (increased stretch), providing further evidence for heterogeneity of bottle cell morphology (Figure 3, C and D).

We further explored differences in the contractile dynamics of round versus fusiform cells and found that rounding cells (decreasing stretch) showed a stronger correlation between medial actin localization and apical area than did fusiform cells (increasing stretch) (Figure 3E). A more notable difference was observed between junctional actin accumulation and apical area reduction, with rounding bottle cells showing much stronger correlation than the fusiform cells (Figure 3F). The subpopulation of cells with a positive correlation between junctional F-actin localization and apical area (Figure 2D, dashed cyan ellipsis) was most clearly visible in fusiform cells (Figure 3F, dashed cyan ellipsis), suggesting that this F-actin behavior may associate with cell stretching. These results indicate that rounding and fusiform bottle cells may employ different mechanisms for apical constriction and cell shape change.

Knockdown of *plekhg5* leads to failure in accumulation of both medioapical and junctional F-actin

Previous studies from our groups have shown that the RhoGEF gene *plekhg5* is required for apical constriction of the bottle cells (Popov *et al.*, 2018). To explore how *plekhg5* may regulate subcellular F-actin dynamics, we injected antisense splicing-blocking *plekhg5* morpholino oligo (MO) together with the RNAs of mem-mCherry and utrophin-GFP into early *Xenopus* embryos. The behaviors of F-actin in the presumptive bottle cells in the morphants were examined at early gastrula stages. Similar to cells in wild-type embryos, F-actin displayed dynamic reorganization at the apical cortex, with the appearance and disappearance of distinct puncta (Supplemental Movies 3 and 4; Figure 4A). However, despite the initial F-actin dynamics, progression toward enrichment of medioapical and junctional F-actin was stalled. As gastrulation proceeded, the intensity of both medial and junctional F-actin diminished over time, and apical constriction was greatly disrupted in *plekhg5* morphants compared with wild-type cells (Supplemental Movies 3 and 4; Figure 4, A–D). F-actin at the cell junctions often displayed periodic intense flares before receding to the normal levels (Figure 4A, arrowheads), a pattern reminiscent of junctional tear and repair (Stephenson *et al.*, 2019). Taken together, the results suggest that *plekhg5* coordinates enhanced F-actin accumulation at both medial and junctional regions to efficiently reduce cell surface and impact cell shape formation.

Coordinated action of myosin and F-actin during bottle cell formation is disrupted in *plekhg5* knockdown cells

The active reduction of apical cell surface requires F-actin and non–muscle type II myosin to form the cytoskeletal contractile network. To investigate how actin and myosin coordinate during apical constriction of the bottle cells, we coinjected RNAs encoding utrophin-RFP and GFP-tagged non–muscle myosin heavy chain IIB (GFP-NMHC-IIB, or myoIIB-GFP) into the dorsal marginal zone of four- to eight-cell-stage embryos. Time-lapse microscopy revealed that like F-actin, MyoIIB was located mainly at the cell junctions before apical constriction. During bottle cell formation, the intensity of both F-actin and MyoIIB signals was increased, with the concurrent reduction of apical surface areas (Supplemental Movies 5 and 6; Figure 5). The enhanced actomyosin signals were concentrated under the apical cell membrane and at the cell junctions. When captured at a later stage of apical constriction when bottle cells had initiated invagination, the greatest actomyosin accumulation was seen to be centered in the medial region of the bottle cells. Both F-actin and MyoIIB formed intense signal patches in the medioapical areas. F-actin could be detected clearly at the cell junctions, while MyoIIB signals at junctions were less distinct compared with their extreme medial enrichment (Supplemental Movie 6; Figure 5, B and C). Apical constriction seemed to have reached its maximal extent by this stage, as cells displayed only nominal changes in apical areas while maintaining strong medioapical actomyosin signals as they invaginated further into the interior of the embryos.

To examine how *plekhg5* regulates coordination between F-actin and myosin, we tracked the dynamics of F-actin and MyoIIB simultaneously in the *plekhg5* morphant embryos (Supplemental Movie 7; Figure 6, A and B). As described above, F-actin displayed dynamic reorganization at the apical cell cortex and formed punctate structures. MyoIIB, however, stayed mainly at the junctions of morphant cells, with only a weak signal observed under the apical membrane. Medial MyoIIB accumulation was also extremely defective in *plekhg5* morphant cells (Figure 6C). Junctional MyoIIB in morphant cells was not uniform and formed discrete patches that were fluid and moved along the cell–cell contacts. Over the course of imaging, *plekhg5* morphant cells failed to increase both medial and junctional MyoIIB localization (Figure 6, C and D). Together these results indicate that Plekhg5 is primarily activating apical constriction through actomyosin recruitment and activation in bottle cells.

DISCUSSION

Apical constriction is a fundamental cellular process employed reiteratively to remodel epithelia during embryogenesis and in adults (Sawyer *et al.*, 2010). Though actomyosin contraction is shown to be a major driving force underlying apical constriction, variations exist in terms of location, timing, and regulation of actomyosin activities as well as the relationship between actomyosin dynamics and cell shape changes during epithelial morphogenesis (Martin and Goldstein, 2014). To gain insight into molecular control of actomyosin contractile machinery during apical constriction, we used the *Xenopus* bottle cells as our model in this study and tracked simultaneously actomyosin behaviors and changes in apical cell areas both in control embryos and in embryos with knockdown of a critical RhoGEF gene, *plekhg5*. Our results demonstrate heterogeneity of bottle cells and uncover an important function of *plekhg5* in organizing the apical actomyosin network.

Heterogeneous morphology of bottle cells around the blastopore lip

Bottle cells form during *Xenopus* gastrulation with drastic shrinkage of apical cell surface, striking apicobasal elongation, and conspicuous expansion of the basal cell compartment to give the cells their distinctive "bottle" shape (Keller, 1981; Hardin and Keller, 1988). Previous SEM studies of en face and sagittal views of the bottle cells provide detailed morphology of these cells, and time-lapse microscopy

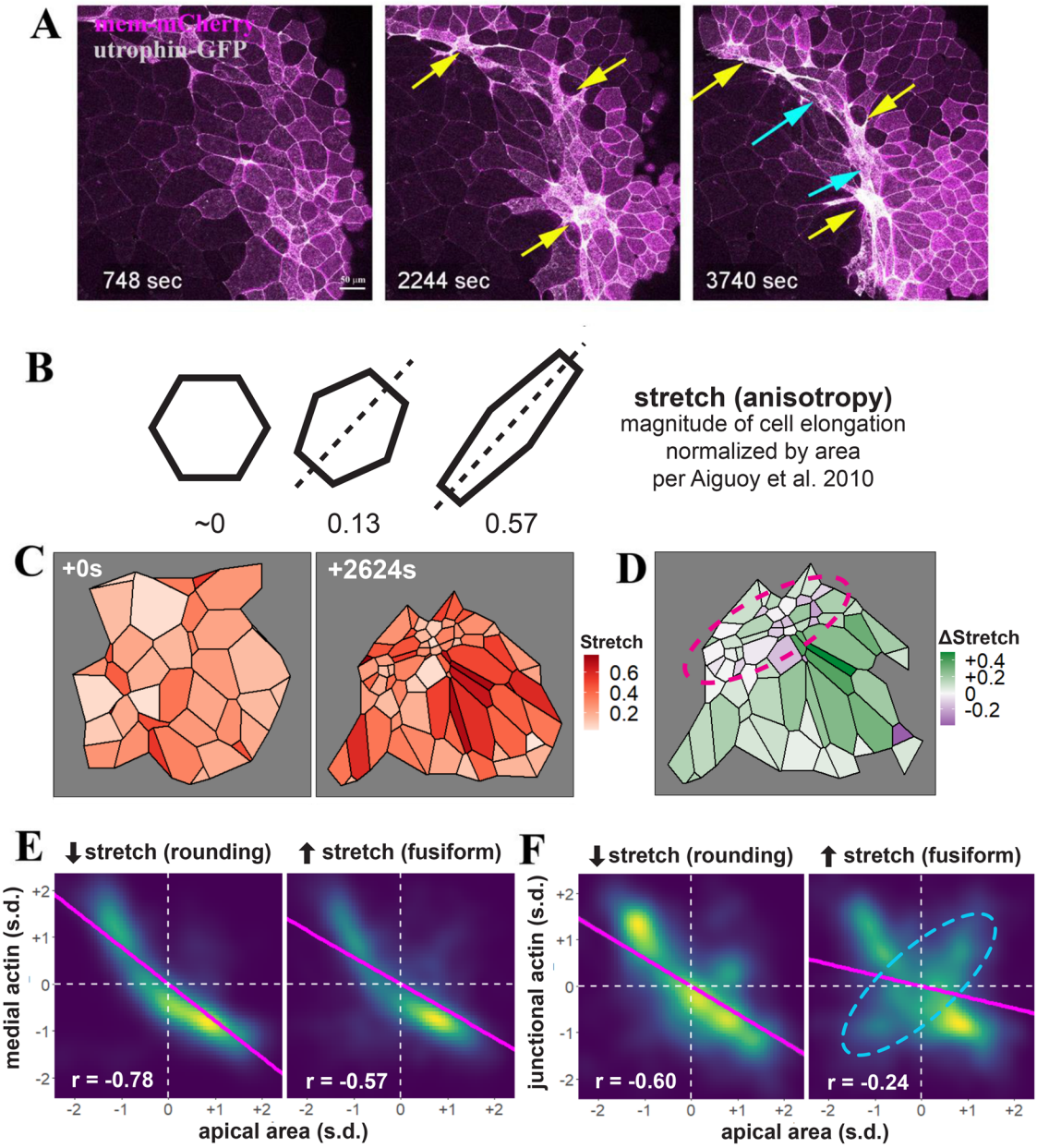

FIGURE 3: Distinct cell shape changes accompany bottle cell formation. (A) Selected frames from a time-lapse movie reveal that apical constriction does not spread from a single point. Clusters of cells some distance apart can constrict around similar times. These cells tend to constrict early and form a round shape (yellow arrows), with the cells in between stretching in the circumferential direction to take the fusiform shape (blue arrows). The bottom yellow arrow in the 3740 s frame points to a constricted cluster of more than 10 cells. (B) Quantification of cell stretch by Tissue Analyzer, whereby the magnitude of cell elongation is normalized by cell area to generate a number ranging from 0 to 1, such that cells with the same shape but different areas will have the same stretch. (C) Example of heterogeneous cell constriction and stretch based on quantitative analysis of a time-lapse movie from the first and the last frames. (D) Mapping of changes of cell stretch onto the embryo images reveals that round, non-stretching cells are juxtaposed to the cells with increasing stretch in the blastopore lip (purple circle). The neighboring cells on the animal pole side of the blastopore lip also display distinct changes in stretch, with cells showing strong stretch preferentially abutting the round bottle cells. (E, F) Quantification of medial (E) or junctional (F) F-actin intensity reveals a stronger correlation with the round bottle cells than with the fusiform bottle cells. A subpopulation of fusiform cells with a positive correlation between junctional F-actin and apical area is labeled with a dashed cyan ellipsis. Magenta line indicates linear model. s.d. = standard deviations. $n = 3171$ observations for cells decreasing stretch (rounding) and 8709 observations for cells increasing stretch (fusiform) collected from four control embryos.

has been used to track bottle cell formation (Keller, 1981; Hardin and Keller, 1988). However, the dynamic process leading to apical cell shape changes in bottle cells had not been fully captured.

Using live imaging to track apical cell surface, we show here that two distinct groups of bottle cells emerge during gastrulation. They differ not only in morphology, with one round

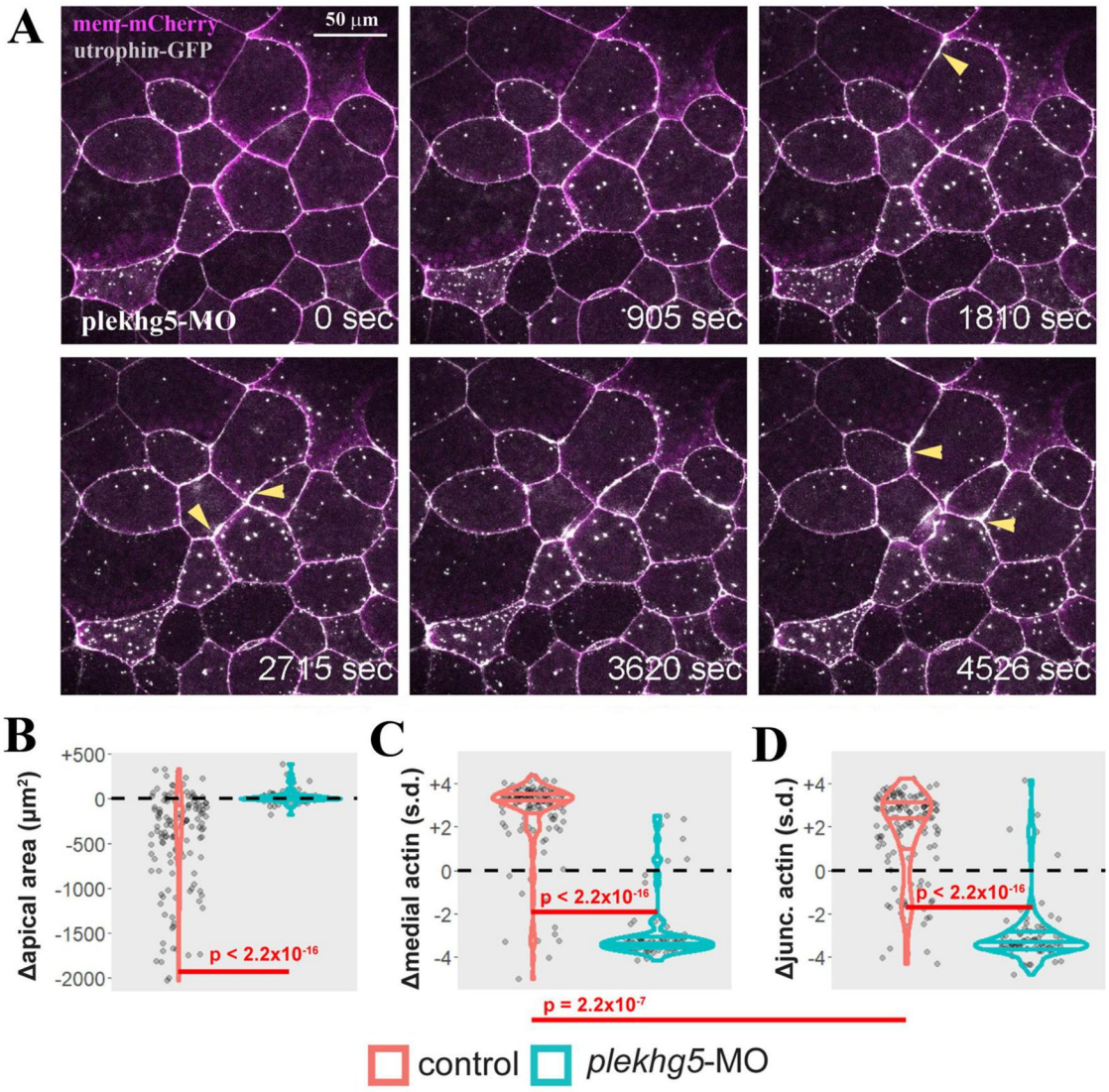

FIGURE 4: Knockdown of *plekhg5* prevents apical accumulation of F-actin and reduction of apical cell size. (A) Selected frames from a time-lapse movie show that despite the initial F-actin dynamics and formation of F-actin puncta, the cells with *plekhg5* knockdown fail to increase apical F-actin signal or reduce the apical surface. Instead, junctional F-actin flares can be seen frequently. The arrowheads point to examples of F-actin flares. (B) Quantification of apical cell area demonstrates that unlike cells in control embryos (Supplemental Movies 1 and 2), cells from *plekhg5* knockdown embryos (Supplemental Movies 3 and 4) cannot reduce their apex efficiently. (C, D) While medial and junctional F-actin intensity increases during apical constriction of bottle cells in control embryos, the intensity of medial and junctional F-actin decreases in cells from *plekhg5* knockdown embryos. Each dot is an individual cell. Horizontal lines within each violin delineate quartiles along each distribution. s.d. = standard deviations. *P* values were calculated via a KS test. Data were collected from four control and five *plekhg5* knockdown embryos.

and the other fusiform in shape, but also in the onset of apical constriction, with the round bottle cells contracting earlier than the fusiform cells. The round, isotropically constricting cells tend to form clusters several cell diameters away and appear to actively reduce their apices autonomously. The fusiform bottle cells initiate their constriction following the round cells and seem to be influenced by their neighboring clusters of isotropically constricting cells to stretch along the circumference of the blastopore.

The heterogeneous populations of bottle cells are apparently required to maintain the circumference of the blastopore, as the circumference would have been diminished once the bottle cells had formed and spread if all cells constricted in an isotropic manner. This would result in premature infolding of the vegetal endoderm and impede the ordered progression of mesendoderm involution. Consistent with the geometric and mechanical constraints of the gastrulating embryos, the cells abutting the bottle cells adopt different shapes as well, with the cells on the animal-pole side to the round bottle cells displaying strong stretching along the animal-vegetal direction, whereas the cells adjacent to the fusiform bottle cells were less stretched (Figure 3, C and D).

Medioapical and junctional actomyosin drives apical constriction

Our quantitative analysis of actomyosin behaviors reveals dynamics across the apical cortex during bottle cell formation. Both junctional

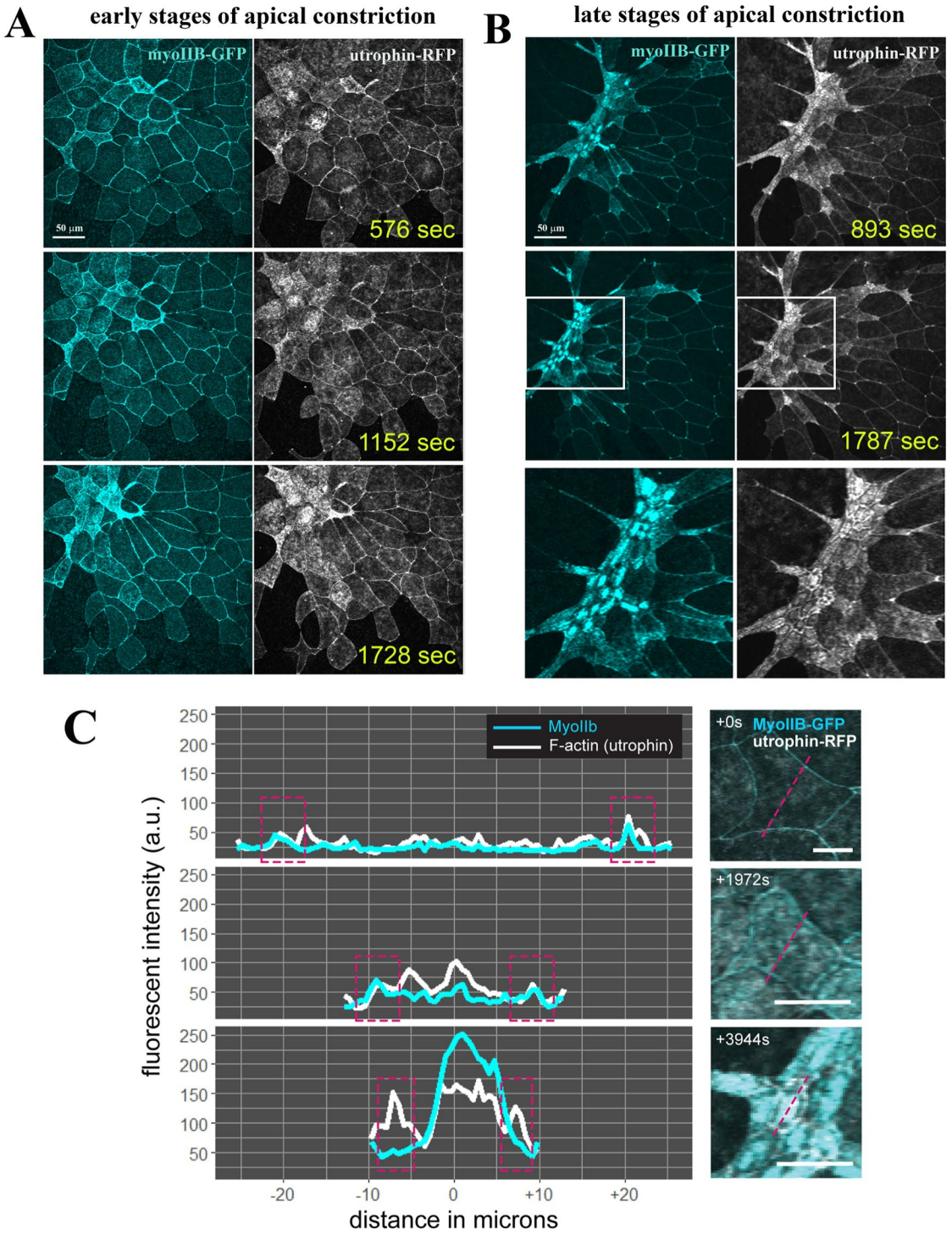

FIGURE 5: Coordinated enrichment of apical myosin IIB and F-actin during apical constriction of bottle cells. (A) Selected frames of a time-lapse movie reveal coordinated increase in MyoIIB and F-actin signals in the apical cortex of the bottle cells. The signal intensity of actomyosin inversely correlates with the apical cell area of the cells. The stretching of neighboring nonconstricting cells can also be seen. (B) During the late stage of apical constriction, the MyoIIB signal is down-regulated from cell junctions and is concentrated in the center of the bottle cells. F-actin signal can be seen in both the cell junctions and the medioapical region. Close-up view of the boxed regions is shown in the bottom panels. (C) Histogram of F-actin and MyoIIB signal intensity at the beginning, in the middle, and at the end of the apical constriction of the bottle cells reveals distinct patterns. While both medial and junctional F-actin and MyoIIB signals increase initially during bottle cell formation, junctional MyoIIB is reduced at the end of apical constriction while junctional F-actin remains strong. Approximate junctional region highlighted by dashed magenta boxes in left panels. Dashed magenta lines in right panels indicate quantified region of each cell.

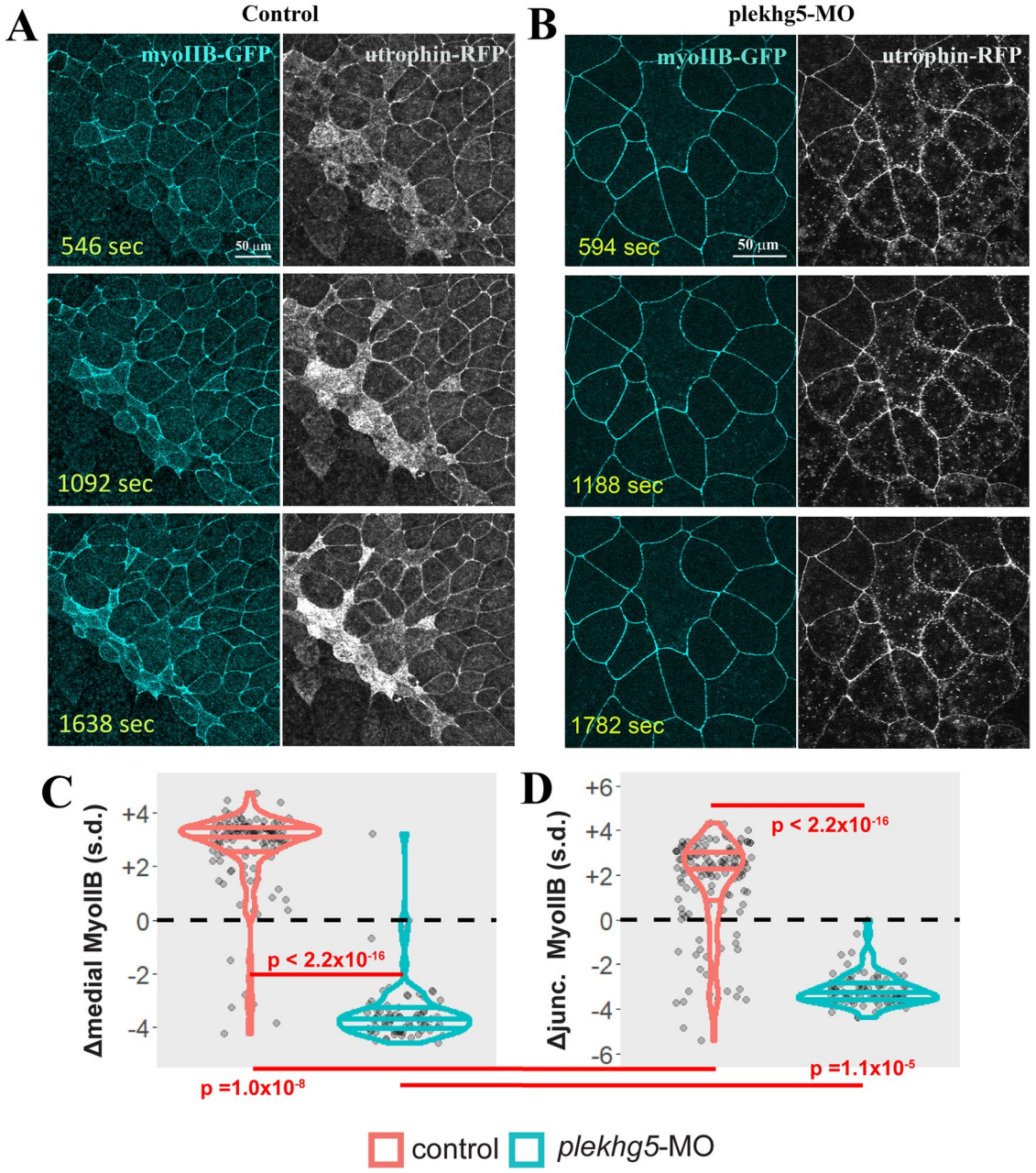

FIGURE 6: Knockdown of *plekhg5* prevents medial accumulation of MyoIIB. (A, B) Unlike cells in control embryos, in *plekhg5* knockdown embryos, initial F-actin dynamics remains in the apical cortex but MyoIIB fails to show up in the medial domain. No actomyosin enrichment is observed with progression of time. (C, D) Quantification of medial and junctional MyoIIB intensity shows that unlike in control bottle cells where the intensity of MyoIIB increases, medial and junctional MyoIIB decrease in cells with *plekhg5* knockdown. Each dot is an individual cell. Horizontal lines within each violin delineate quartiles along each distribution. s.d. = standard deviations. *P* values were calculated via a KS test. Data were collected from four control and five *plekhg5* knockdown embryos.

and medial actomyosin signals increase as the apical surface area is reduced, though the strongest enhancement of actomyosin intensity and the higher correlation coefficient scores are seen in the medial domain. The deployment of medioapical actomyosin may provide several features consistent with bottle cell biology.

First, medial contractility could better enable the cell-autonomous asynchronous contraction seen in the clusters of bottle cells some distance apart. Junctional actomyosin contractility may transmit tension to all of a cell's neighbors during constriction, thus favoring the spreading of constriction continuously around the circumference, a phenomenon inconsistent with our observation of the spaced-out clusters of cells that independently initiate constriction during blastopore lip formation (Figure 3A). We have recently modeled non–cell autonomous inputs to apical constriction in the neural ectoderm and found that increasing junctional F-actin localization in neighboring cells inhibits apical constriction in a given cell (Baldwin *et al.*, 2022b), lending further weight to this hypothesis.

Second, both endocytosis of the surface membrane and generation of microvilli can reduce the apical area (Keller, 1981; Hardin and Keller, 1988; Kurth and Hausen, 2000; Lee and Harland, 2010), and

we have observed emerging F-actin bundles perpendicular to the apical membrane even before large-scale reduction of the cell apex. The F-actin bundles become especially dense as bottle cells take their mature shape. It thus appears that one main task of medioapical actomyosin is to generate and maintain high-density orthogonal F-actin bundles at the apical cell surface to facilitate apical constriction. Junctional actomyosin would theoretically be less efficient in producing cortical forces to generate dense perpendicular F-actin in the apical compartment. Over the period of our observation, the bottle cells invaginate slightly into the interior of the embryos and junctional myosin is seen to be down-regulated, whereas the medial myosin remains exceedingly strong (Figure 5). This disconnection between medial and junctional myosin may help to reduce junctional tension without relaxing the apical cell area so that epithelial sheet integrity can be preserved as the bottle cells maintain their shapes during mesendoderm involution before they respread at the end of gastrulation (Keller, 1981; Hardin and Keller, 1988).

Third, the level of medial versus junctional actomyosin activities may determine whether cells adopt round or fusiform morphology. While medial actomyosin accumulation correlates with apical area in both round and fusiform bottle cells, junctional actomyosin more strongly correlates area in cells that become rounder (Figure 3). This may be due to the asymmetric junctional tension experienced by the late-forming fusiform bottle cells, whereby high tension exerted by neighboring round cells dominates junctional actomyosin activities over those at the junctions nonadjacent to the round cells. The heterogeneity in junctional actomyosin in fusiform cells would negatively impact its correlation with apical area.

plekhg5 controls apical actomyosin accumulation to initiate apical constriction in bottle cells

The timing of concentrated actomyosin activities and the apical localization of the contractile meshwork need to be regulated tightly to allow accurate and reproducible morphogenesis. Many regulators of apical constriction have been reported in different tissue contexts and/or organisms, with the factors controlling the actions of the Rho family small GTPases among the prominent ones. The *Drosophila* DRhoGEF2 and the vertebrate GEF-H1/Arhgef2, which stimulate RhoA activation, are shown to act in the apical domain to promote actomyosin assembly and facilitate apical constriction (Barrett *et al.*, 1997; Hacker and Perrimon, 1998; Nikolaidou and Barrett, 2004; Itoh *et al.*, 2014). Conversely, the Cdc42 GAP protein PAC-1, which acts to inactivate Cdc42, is reported to function in the basolateral regions of *C. elegans* endodermal cells to limit Cdc42 activity only to the apical domain (Lee and Goldstein, 2003; Anderson *et al.*, 2008; Chan and Nance, 2013; Marston *et al.*, 2016). In *Xenopus*, we have previously identified a RhoGEF gene, *plekhg5*, that regulates apical constriction of bottle cells in a RhoA-dependent manner (Popov *et al.*, 2018). Plekhg5 is located in the apical domain, and its activity is required for actomyosin accumulation underneath the apical membrane. However, how *plekhg5* controls actomyosin dynamics has not been described.

In this study, we show that knockdown of *plekhg5* does not affect initial F-actin dynamics in the apical cortex, as active formation and dissolution of F-actin punctate can be observed in the absence of *plekhg5*. This suggests that other regulators exist to stimulate F-actin remodeling when gastrulation starts. However, *plekhg5* is crucial for maintaining and enhancing actomyosin activities in bottle cells. Both medioapical and junctional actomyosin signals are reduced with time when *plekhg5* is knocked down. It is likely that Plekhg5 carries out the task via downstream effectors of activated RhoA, including ROCK and Dia (Narumiya *et al.*, 2009). ROCK can phosphorylate regulatory MLC to activate myosin contractility, whereas Dia is a formin domain–containing protein that can promote actin bundle formation. Apically localized Plekhg5 can therefore stimulate local assembly and contraction of actomyosin to facilitate reduction of the apical surface area. It is interesting to note that while *plekhg5* is expressed in cells around the blastopore lip, not all the blastopore lip cells express *plekhg5* at the same time. Instead, the gene is expressed in a salt-and-pepper manner in subsets of the cells in the lip region (Supplemental Figure 2). Considering that we observe the round and the fusiform bottle cells that differ in temporal onset and possibly autonomy in force generation, we propose that *plekhg5*-expressing cells may initiate isotropic apical constriction in discrete cells that contributes to early-forming round bottle cells, whereas the *plekhg5*-nonexpressing cells constrict later and take the fusiform shape. Knockdown of *plekhg5* would prevent the formation of both types of bottle cells, as fusiform cells seem to depend on the appearance of round cells. Though this model is consistent with our data, we do not have direct evidence currently.

Plekhg5 and Shroom3 are mechanistically distinct activators of apical constriction during *Xenopus* embryogenesis

Comparing apical constriction in the context of neural tube closure in *Xenopus* (Baldwin *et al.*, 2022a), we find both common and unique features. In both bottle cells and cells within the neural plate, medioapical and junctional actomyosin appear to provide driving forces for apical constriction. However, the mechanisms of actomyosin regulation seem to differ between these tissues. As we have shown previously (Baldwin *et al.*, 2022a), the actin-binding protein Shroom3 is a critical regulator of apical constriction in neural ectoderm cells. Shroom3 controls N-cadherin localization and coupling of actin contraction to effectively reduce apical surface area. Mutation of *shroom3* does not entirely prevent medial actin accumulation but precludes actin-driven reduction of the apical surface area. In comparison, none of the *shroom* family genes is expressed in bottle cells by in situ hybridization analysis (Lee *et al.*, 2009). Apical constriction of bottle cells therefore appears to proceed independent of *shroom* function and relies on the activity of the RhoGEF gene *plekhg5*.

Unlike in *shroom3*-depleted cells, actin fails to accumulate in either medial or junctional regions in *plekhg5* knockdown cells. This suggests that *plekhg5* plays a more fundamental role than *shroom3* in the assembly of the apical actomyosin network. As both Shroom3 and Plekhg5 are apically localized and can activate ROCK via either direct binding to ROCK or Rho activation (Ngok and Anastasiadis, 2013; Das *et al.*, 2014; Mack and Georgiou, 2014), the difference in their function in regulating apical actin accumulation may reflect other distinct partners and downstream effectors of these two factors. Identification of molecular components involved in the control of apical constriction by Shroom3 and Plekhg5 can provide valuable information on distinct mechanisms regulating an important cellular process underlying epithelial morphogenesis.

In summary, we show in this study that bottle cells are not homogeneous and take different shapes. The formation of bottle cells relies on medioapical and junctional actomyosin meshwork, and the RhoGEF protein Plekhg5 is essential for enhancing actomyosin activity so that apical constriction can proceed to generate epithelial deformation during *Xenopus* gastrulation. Though the contractile actomyosin meshwork seems to be a shared feature of apical constriction with many other species, F-actin bundles perpendicular to the apical surface that may associate with the formation of microvilli appear to be more specific for reducing the large surface area in the bottle cells of *Xenopus*. It will be interesting to investigate in the future whether fusiform bottle cells constrict actively or passively,

how remodeling of junctional adhesion complexes contributes to reduction of apical surface area, what functions of Rho effectors ROCK and Dia play during bottle cell formation, and how Plekhg5 expression and activity are regulated by other signals involved in cell fate determination and morphogenesis.

MATERIALS AND METHODS

Request a protocol through *Bio-protocol*.

Embryo culture and injection

Xenopus laevis frogs were used under institutional IACUC protocol 21371 at the University of Alabama at Birmingham. The embryos were obtained by in vitro fertilization. The GFP-MyoIIB construct was obtained from Addgene (Addgene plasmid #11348) (Wei and Adelstein, 2000) and cloned into the pCS105 vector. The membrane mCherry and utrophin-GFP/RFP plasmids were used as described before (Burkel *et al.*, 2007). RNAs were synthesized from the linearized plasmids using the in vitro mMessage mMachine RNA synthesis kit (Ambion). Mem-mCherry and utrophin-GFP/RFP RNAs (100–250 pg) and 1–2 ng of myoIIB-GFP RNAs were injected into the marginal zone regions of two dorsal blastomeres of four- to eight-cell-stage embryos. The embryos were imaged around the time just before and immediately after the dorsal lip appears, from the late blastula to early gastrula stages. Half the injected embryos were cultured to the tailbud-to-tadpole stages to ensure that the injected RNAs did not affect the embryo development. For *plekhg5* knockdown, a previously tested antisense splicing-blocking MO (Popov *et al.*, 2018) was used at a total of 25–33 ng into the dorsal marginal zone of four-cell-stage embryos.

Imaging of actomyosin dynamics in the bottle cells

The injected embryos were collected at late blastula stages, with their vitelline membrane removed, and imaged with either an upright Olympus Fluoview F1000, inverted Nikon A1R confocal microscopes, or a Zeiss LSM900 Airyscan microscope. To prevent embryos from sticking to the cover glasses or imaging dishes, the glasses and the dishes were treated with 1% bovine serum albumin. The embryos were positioned with the presumptive dorsal lip region in the imaging view. Time-lapse microscopy was performed with z-stack to cover the entire curved surface in view and no pause in between time points (continuous run). This would end up with images with 4–17 z-stacks and a time interval of about 16–22 s. Maximum-intensity projection was carried out using FIJI, and the resulting movies are included in the Supplemental Materials. For phalloidin staining, gastrula embryos fixed in MEMFA (MOPS/EGTA/Magnesium Sulfate/Formaldehyde Buffer) were cultured with 5 U/ml AF488-conjugated phalloidin at 4°C overnight before being washed extensively with phosphate-buffered saline and mounted in imaging dishes for Airyscan imaging with a Zeiss LSM900 microscope. An optimal z-section step of 0.2 µm was used for the scan, and the 3D projection of the image stacks was performed using Zeiss Zen Blue software.

Quantitative image analysis

Cells were segmented and tracked using EPySeg, and then EPySeg outputs were manually corrected using Tissue Analyzer (Aigouy *et al.*, 2010, 2016, 2020). Tissue Analyzer was used to break the apical surfaces of cells into two domains: a "medial" domain that encompasses the apical surface within the cell–cell junctions, and a "junctional" domain that is composed solely of the cell–cell junctions (Figure 2B). Tissue Analyzer and FIJI (Schindelin *et al.*, 2012) were further used to calculate mean fluorescence intensities and physical size parameters at each of these domains. Tissue Analyzer databases were imported to R and further analyzed and manipulated primarily using the tidyverse package (Wickham *et al.*, 2019; R Core Team, 2020). Frame intervals for each movie varied slightly, ranging from 16 to 22 s, so parameters within each cell were averaged over a seven-frame window to account for "noise" within our measurements. To account for differences in initial size and intensity of fluorescent markers, parameters were standardized by mean centering the data for each individual cell track to zero and then dividing the resulting mean-centered values by the standard deviation of each track. Thus, parameters are displayed in both standard deviations and square microns or arbitrary units, allowing for relative dynamics to be compared between cells in addition to raw changes in parameters (Baldwin *et al.*, 2022a). Kolmogorov–Smirnov (KS) tests were performed using the ks.test function in R. Data used in generation of the above figures can be found in the Supplemental Excel files in Supplemental Data section of this article.

For measuring the lengths of F-actin bundles, the 3D-projected images were viewed with F-actin bundles in vertical positions and their lengths and the length of *z*-axial coordinates in microns were measured using the FIJI software. The lengths of F-actin bundles in microns were then calculated. For the apical cell areas, the visible cell areas were measured and converted into square microns using the reference area from the *X* and *Y* coordinates. Only partial cells were included in some images; hence the exact apical areas could not be obtained from these images. The cells were therefore grouped to two with areas greater or less than 50 square microns. Totals of five-early and four late-stage embryos were analyzed in this study.

ACKNOWLEDGMENTS

The work is supported by National Institutes of Health (NIH) Grants R01 GM127371 (C. C. and R. K.) and R01HD099191 (J. W.) and NIH fellowship F32 HD094521 (A. B.).

REFERENCES

Aigouy B, Cortes C, Liu S, Prud'Homme B (2020). EPySeg: a coding-free solution for automated segmentation of epithelia using deep learning. Development 147, dev194589.

Aigouy B, Farhadifar R, Staple DB, Sagner A, Roper JC, Julicher F, Eaton S (2010). Cell flow reorients the axis of planar polarity in the wing epithelium of Drosophila. Cell 142, 773–786.

Aigouy B, Umetsu D, Eaton S (2016). Segmentation and quantitative analysis of epithelial tissues. Methods Mol Biol 1478, 227–239.

An Y, Xue G, Shaobo Y, Mingxi D, Zhou X, Yu W, Ishibashi T, Zhang L, Yan Y (2017). Apical constriction is driven by a pulsatile apical myosin network in delaminating Drosophila neuroblasts. Development 144, 2153–2164.

Anderson DC, Gill JS, Cinalli RM, Nance J (2008). Polarization of the C. elegans embryo by RhoGAP-mediated exclusion of PAR-6 from cell contacts. Science 320, 1771–1774.

Baldwin AT, Kim J, Seo H, Wallingford JB (2022a). Global analysis of cell behavior and protein localization dynamics reveals region-specific functions for Shroom3 and N-cadherin during neural tube closure. eLife 11, e66704.

Baldwin AT, Kim JH, Wallingford JB (2022b). In vivo high-content imaging and regression analysis reveal non-cell autonomous functions of Shroom3 during neural tube closure. Dev Biol 491, 105–112.

Barrett K, Leptin M, Settleman J (1997). The Rho GTPase and a putative RhoGEF mediate a signaling pathway for the cell shape changes in Drosophila gastrulation. Cell 91, 905–915.

Bement WM, Forscher P, Mooseker MS (1993). A novel cytoskeletal structure involved in purse string wound closure and cell polarity maintenance. J Cell Biol 121, 565–578.

Blanchard GB, Murugesu S, Adams RJ, Martinez-Arias A, Gorfinkiel N (2010). Cytoskeletal dynamics and supracellular organisation of cell shape fluctuations during dorsal closure. Development 137, 2743–2752.

Booth AJR, Blanchard GB, Adams RJ, Roper K (2014). A dynamic microtubule cytoskeleton directs medial actomyosin function during tube formation. Dev Cell 29, 562–576.

Burkel BM, von Dassow G, Bement WM (2007). Versatile fluorescent probes for actin filaments based on the actin-binding domain of utrophin. Cell Motil Cytoskeleton 64, 822–832.
Chan E, Nance J (2013). Mechanisms of CDC-42 activation during contact-induced cell polarization. J Cell Sci 126, 1692–1702.
Chanet S, Miller CJ, Vaishnav ED, Ermentrout B, Davidson LA, Martin AC (2017). Actomyosin meshwork mechanosensing enables tissue shape to orient cell force. Nat Commun 8, 15014.
Choi SC, Sokol SY (2009). The involvement of lethal giant larvae and Wnt signaling in bottle cell formation in Xenopus embryos. Dev Biol 336, 68–75.
Christodoulou N, Skourides PA (2015). Cell-autonomous Ca(2+) flashes elicit pulsed contractions of an apical actin network to drive apical constriction during neural tube closure. Cell Rep 13, 2189–2202.
Chung S, Kim S, Andrew DJ (2017). Uncoupling apical constriction from tissue invagination. eLife 6, e22235.
Das D, Zalewski JK, Mohan S, Plageman TF, VanDemark AP, Hildebrand JD (2014). The interaction between Shroom3 and Rho-kinase is required for neural tube morphogenesis in mice. Biol Open 3, 850–860.
Goldstein B, Nance J (2020). Caenorhabditis elegans gastrulation: a model for understanding how cells polarize, change shape, journey toward the center of an embryo. Genetics 214, 265–277.
Hacker U, Perrimon N (1998). DRhoGEF2 encodes a member of the Dbl family of oncogenes and controls cell shape changes during gastrulation in Drosophila. Genes Dev 12, 274–284.
Hardin J, Keller R (1988). The behaviour and function of bottle cells during gastrulation of Xenopus laevis. Development 103, 211–230.
Itoh K, Ossipova O, Sokol SY (2014). GEF-H1 functions in apical constriction and cell intercalations and is essential for vertebrate neural tube closure. J Cell Sci 127, 2542–2553.
Jodoin JN, Coravos JS, Chanet S, Vasquez CG, Tworoger M, Kingston ER, Perkins LA, Perrimon N, Martin AC (2015). Stable force balance between epithelial cells arises from F-actin turnover. Dev Cell 35, 685–697.
Kamran Z, Zellner K, Kyriazes H, Kraus CM, Reynier JB, Malamy JE (2017). In vivo imaging of epithelial wound healing in the cnidarian Clytia hemisphaerica demonstrates early evolution of purse string and cell crawling closure mechanisms. BMC Dev Biol 17, 17.
Keller RE (1981). An experimental analysis of the role of bottle cells and the deep marginal zone in gastrulation of Xenopus laevis. J Exp Zool 216, 81–101.
Kiehart DP, Crawford JM, Aristotelous A, Venakides S, Edwards GS (2017). Cell sheet morphogenesis: dorsal closure in Drosophila melanogaster as a model system. Annu Rev Cell Dev Biol 33, 169–202.
Ko CS, Tserunyan V, Martin AC (2019). Microtubules promote intercellular contractile force transmission during tissue folding. J Cell Biol 218, 2726–2742.
Kurth T (2005). A cell cycle arrest is necessary for bottle cell formation in the early Xenopus gastrula: integrating cell shape change, local mitotic control and mesodermal patterning. Mech Dev 122, 1251–1265.
Kurth T, Hausen P (2000). Bottle cell formation in relation to mesodermal patterning in the Xenopus embryo. Mech Dev 97, 117–131.
Lang RA, Herman K, Reynolds AB, Hildebrand JD, Plageman TF Jr (2014). p120-catenin-dependent junctional recruitment of Shroom3 is required for apical constriction during lens pit morphogenesis. Development 141, 3177–3187.
Le TP, Chung S (2021). Regulation of apical constriction via microtubule- and Rab11-dependent apical transport during tissue invagination. Mol Biol Cell 32, 1033–1047.
Lee C, Le MP, Wallingford JB (2009). The shroom family proteins play broad roles in the morphogenesis of thickened epithelial sheets. Dev Dyn 238, 1480–1491.
Lee C, Scherr HM, Wallingford JB (2007). Shroom family proteins regulate gamma-tubulin distribution and microtubule architecture during epithelial cell shape change. Development 134, 1431–1441.
Lee JY, Goldstein B (2003). Mechanisms of cell positioning during C. elegans gastrulation. Development 130, 307–320.
Lee JY, Harland RM (2007). Actomyosin contractility and microtubules drive apical constriction in Xenopus bottle cells. Dev Biol 311, 40–52.
Lee JY, Harland RM (2010). Endocytosis is required for efficient apical constriction during Xenopus gastrulation. Curr Biol 20, 253–258.
Mack NA, Georgiou M (2014). The interdependence of the Rho GTPases and apicobasal cell polarity. Small GTPases 5, 10.
Marston DJ, Higgins CD, Peters KA, Cupp TD, Dickinson DJ, Pani AM, Moore RP, Cox AH, Kiehart DP, Goldstein B (2016). MRCK-1 drives apical constriction in C. elegans by linking developmental patterning to force generation. Curr Biol 26, 2079–2089.
Martin AC, Goldstein B (2014). Apical constriction: themes and variations on a cellular mechanism driving morphogenesis. Development 141, 1987–1998.
Martin AC, Kaschube M, Wieschaus EF (2009). Pulsed contractions of an actin-myosin network drive apical constriction. Nature 457, 495–499.
Mason FM, Tworoger M, Martin AC (2013). Apical domain polarization localizes actin-myosin activity to drive ratchet-like apical constriction. Nat Cell Biol 15, 926–936.
Massarwa R, Schejter ED, Shilo BZ (2009). Apical secretion in epithelial tubes of the Drosophila embryo is directed by the Formin-family protein Diaphanous. Dev Cell 16, 877–888.
Mulinari S, Barmchi MP, Hacker U (2008). DRhoGEF2 and diaphanous regulate contractile force during segmental groove morphogenesis in the Drosophila embryo. Mol Biol Cell 19, 1883–1892.
Nakajima H, Tanoue T (2011). Lulu2 regulates the circumferential actomyosin tensile system in epithelial cells through p114RhoGEF. J Cell Biol 195, 245–261.
Nakajima H, Tanoue T (2012). The circumferential actomyosin belt in epithelial cells is regulated by the Lulu2-p114RhoGEF system. Small GTPases 3, 91–96.
Narumiya S, Tanji M, Ishizaki T (2009). Rho signaling, ROCK and mDia1, in transformation, metastasis and invasion. Cancer Metastasis Rev 28, 65–76.
Ngok SP, Anastasiadis PZ (2013). Rho GEFs in endothelial junctions: effector selectivity and signaling integration determine junctional response. Tissue Barriers 1, e27132.
Nikolaidou KK, Barrett K (2004). A Rho GTPase signaling pathway is used reiteratively in epithelial folding and potentially selects the outcome of Rho activation. Curr Biol 14, 1822–1826.
Ossipova O, Chuykin I, Chu CW, Sokol SY (2015). Vangl2 cooperates with Rab11 and Myosin V to regulate apical constriction during vertebrate gastrulation. Development 142, 99–107.
Plageman TF Jr, Chauhan BK, Yang C, Jaudon F, Shang X, Zheng Y, Lou M, Debant A, Hildebrand JD, Lang RA (2011). A Trio-RhoA-Shroom3 pathway is required for apical constriction and epithelial invagination. Development 138, 5177–5188.
Popov IK, Ray HJ, Skoglund P, Keller R, Chang C (2018). The RhoGEF protein Plekhg5 regulates apical constriction of bottle cells during gastrulation. Development 145, dev168922.
R Core Team (2020). R: A Language and Environment for Statistical Computing, Vienna, Austria: R Foundation for Statistical Computing.
Rogers SL, Wiedemann U, Hacker U, Turck C, Vale RD (2004). Drosophila RhoGEF2 associates with microtubule plus ends in an EB1-dependent manner. Curr Biol 14, 1827–1833.
Roh-Johnson M, Shemer G, Higgins CD, McClellan JH, Werts AD, Tulu US, Gao L, Betzig E, Kiehart DP, Goldstein B (2012). Triggering a cell shape change by exploiting preexisting actomyosin contractions. Science 335, 1232–1235.
Rousso T, Shewan AM, Mostov KE, Schejter ED, Shilo BZ (2013). Apical targeting of the formin Diaphanous in Drosophila tubular epithelia. eLife 2, e00666.
Sawyer JM, Harrell JR, Shemer G, Sullivan-Brown J, Roh-Johnson M, Goldstein B (2010). Apical constriction: a cell shape change that can drive morphogenesis. Dev Biol 341, 5–19.
Schindelin J, Arganda-Carreras I, Frise E, Kaynig V, Longair M, Pietzsch T, Preibisch S, Rueden C, Saalfeld S, Schmid B, *et al*. (2012). Fiji: an open-source platform for biological-image analysis. Nat Methods 9, 676–682.
Simoes S, Mainieri A, Zallen JA (2014). Rho GTPase and Shroom direct planar polarized actomyosin contractility during convergent extension. J Cell Biol 204, 575–589.
Simões S, Oh Y, Wang MFZ, Fernandez-Gonzalez R, Tepass U (2017). Myosin II promotes the anisotropic loss of the apical domain during Drosophila neuroblast ingression. J Cell Biol 216, 1387–1404.
Stephenson RE, Higashi T, Erofeev IS, Arnold TR, Leda M, Goryachev AB, Miller AL (2019). Rho flares repair local tight junction leaks. Dev Cell 48, 445–459.e445.
Wei Q, Adelstein RS (2000). Conditional expression of a truncated fragment of nonmuscle myosin II-A alters cell shape but not cytokinesis in HeLa cells. Mol Biol Cell 11, 3617–3627.
Wickham H, Averick M, Bryan J, Chang W, D'Agostino McGowan L, François R, Grolemund G, Hayes A, Henry L, Hester J, *et al*. (2019). Welcome to the Tidyverse. J Open Source Softw 4, 1686.
Yano T, Tsukita K, Kanoh H, Nakayama S, Kashihara H, Mizuno T, Tanaka H, Matsui T, Goto Y, Komatsubara A, *et al*. (2021). A microtubule-LUZP1 association around tight junction promotes epithelial cell apical constriction. EMBO J 40, e104712.